T. Methling, M. Braun-Unkhoff, U. Riedel, An Optimised Chemical Kinetic Model for the Combustion of Fuel Mixtures of Syngas and Natural Gas, Fuel 262 (2020) 116611.

The original publication is available at www.elsevier.com

http://dx.doi.org/10.1016/j.fuel.2019.116611

An Optimised Chemical Kinetic Model for the Combustion of Fuel Mixtures of Syngas and Natural Gas

T. Methling[a,*], M. Braun-Unkhoff[a], U. Riedel[a]

[a] *German Aerospace Center (DLR), Institute of Combustion Technology, 70569 Stuttgart, Germany*

Abstract

A chemical kinetic model for the combustion of fuel mixtures – mainly of hydrogen, carbon monoxide and methane – was derived from a comprehensive optimisation based on experimental data. The experimental data include ignition delay times from shock tubes, species profiles from shock tubes, jet stirred reactors, flow reactors and burner stabilised flames as well as several laminar flame speeds. For this large scale optimisation of 475 model parameters within their uncertainty boundaries the novel linear transformation model was successfully applied. The derived optimised chemical kinetic model reproduces the experimental data significantly more accurately than established conventional models that are also investigated in this study. In this regard, especially the reproducibility of the experiments for the combustion of fuel mixtures containing both syngas and methane is significantly increased. The chemical kinetic model is valid for a wide range of boundary conditions and is suitable for the numerical design and adaptation of various combustion machinery running on the investigated fuel mixtures or biogenic

*Corresponding author:
Email address: torsten.methling@dlr.de (T. Methling)

gases, respectively.

Keywords:

chemical kinetic model, syngas, natural gas, biogenic fuel, optimisation

---

1. Introduction

The accurate chemical kinetic modelling of H_2, CO and CH_4 combustion is of vast importance. On the one hand these fuel components are typical for biogenic gas mixtures, which gain more attention for combustion machinery and are for instance utilised in decentralised power generation. On the other hand the combustion model of these components is the basis of any chemical kinetic model of more complex hydrocarbons. Thus, accurate chemical kinetic models are required for sophisticated designs of combustion machinery to guarantee reliable and safe operation of the machinery at low pollutant emissions. Whereas many reliable chemical kinetic models have been developed for the combustion of syngas and methane (e.g. [1–3]), these models still show some discrepancies on the numerical reproduction of many fundamental experiments, especially for fuel mixtures of syngas and methane, e.g. for shock tubes [4], for jet stirred reactors [5] or laminar burners [6]. A reason for these discrepancies can be certain chemical kinetic processes that are not fully included in the current models, which can lead to systematic errors in simulations. An example of such processes are reactions forming HCO. HCO has a relatively low dissociation threshold. As a consequence, the timescales of vibrational and rotational relaxation and dissociation are comparable [7]. This can lead to a prompt dissociation of HCO radicals formed by reactions, which can have a strong influence on chemical kinetic processes and signifi-

cantly impact combustion characteristics like laminar flame speeds [7, 8].

Another main reason for model deficiencies is the large number of hundreds or thousands of model parameters – mainly parameters of reaction rate coefficients – and their uncertainties from the direct determination of the parameter coefficients via experiments or numerical simulations [9]. To improve the chemical kinetic models, hyperdimensional model optimisations based on large data sets derived from combustion experiments can be applied. Thereby, extensive optimisations of chemical kinetic models were successfully performed and documented in the literature, e.g. for the combustion of hydrogen [10–12], syngas [13] or natural gas [1, 14]. These optimisations were mainly based on response surface methods, which approximate the solution space of the hyperdimensional model parameters by polynomials. For this approximation a large number of randomised model parameter sets need to be evaluated. Thereby, the computational costs of this approximation increases exponentially with the number of optimised model parameters, drastically limiting the efficiency of research in this field of optimisation. To overcome this limitation, the novel linear transformation model (linTM) can be applied [15]. With the linTM the relations between model parameters and output parameters of the solution space are linearised, at the same time keeping a high accuracy of this linear approximation. Hereby, the numerical costs are radically decreased compared to conventional methods, as the increase of the numerical costs is not exponentially but linearly dependent on the number of optimised model parameters. This approach is very general and can be applied with data from various fundamental experiments and for a broad variety of fuels.

The objective of this work is the optimisation of a large number of chemical kinetic model parameters (more than 400) to increase the reproducibility of experimental results from the combustion of fuel mixtures, consisting mainly of syngas and methane. Hereby, model parameters are optimised within their uncertainty limits gained from literature. With the optimisation, a wide range of experimental data was targeted, including ignition delay times, species profiles and laminar flame speeds. Indications are given towards modelling directions for further investigation on certain reaction rate coefficients. Though, one major drawback of these optimisation processes is the inability to detect or account for systematic errors. A past example of these errors from models is the afore mentioned prompt dissociation of HCO. Due to the complexity and high number of model parameters in chemical kinetic models for the investigated combustion processes, the reduction of uncertainty bands of rate coefficients is not a major objective of this work. Thus, the main purpose of the optimised model is to increase the prediction accuracy e.g. of CFD simulations for the design and adaptation of applied reliable combustion machinery at low pollutant emission levels.

2. Optimisation Method

The linear transformation model (linTM) – including its optimisation method – is described in detail in prior work [15] and is only reviewed briefly here. The linTM mainly consists of two basic concepts. On the one hand the Arrhenius coefficients are substituted by a set of three different input parameters. In detail the first two parameters to represent the Arrhenius equation are two deviations from the original rate coefficient at two different temper-

atures $\Delta \lg(k(T_1))$ and $\Delta \lg(k(T_2))$. In addition, for the full parametrisation of the Arrhenius equation a third parameter is required. This parameter is either a third deviation of the original rate coefficient $\Delta \lg(k(T_3))$ or a deviation from the original activation energy ΔE_A. With this substitution, the dependencies of the input parameters on each other are decoupled. To simplify the mathematical notations, all input parameters are represented by normalised variables τ_i. On the other hand species profiles (as a function of time, distance or temperature) or laminar flame speed profiles (as a function of the fuel-air equivalence ratio φ) are defined by coordinates of characteristic points (CP), e.g. the maximum of an intermediate or the point where 50% of the maximum value is reached. Hereby, experiment and simulation results are compared by distances d_j between these coordinates or the quantities q, respectively:

$$d_j = \ln\left(\frac{q_{j,\mathrm{simulation}}}{q_{j,\mathrm{experiment}}}\right). \tag{1}$$

With the linTM the relations between the input parameters and the distances between the coordinates d_j are linearised, thereby, keeping a high accuracy. These simplified linear relations can be efficiently used for the global sensitivity analysis and optimisation of chemical kinetic models. Specifically, for the optimisation, a gradient based solver is applied, using the method of least squares to minimise the distances d_j. For this minimisation, the objective function F is:

$$F = \sum_{j=1}^{D} (w_j d_j)^2, \tag{2}$$

for which, D is the total number of distances. In Eq. (2), the distances are additionally weighted with a weighting factor w_j.

For the sensitivity analysis of a reaction r on the experimental set, we

use the definition of the global sensitivity S_r of the linTM [15]:

$$S_r = \sum_{j=1}^{D} S_{r,j} = \sum_{j=1}^{D} \left(\sum_{i=m}^{m+P_r-1} \left(w_j \frac{\partial d_j}{\partial \tau_i} \right)^2 \right)^{0.5} . \quad (3)$$

In this equation S_r is the sum of the sensitivities of each reaction r on each distance d_j. Thereby, P_r is the total number of input parameters τ_i belonging to reaction r.

3. Selection of Experimental Data

The set of experimental targets for the optimisation process was built from ignition delay times and species profiles from shock tubes (ST), jet stirred reactors (JSR), flow reactors (FR) and burner stabilised flames (BF), and from laminar flame speeds (FS). In this study, experimental data from rapid compression machines (RCM) and species profiles in low pressure flames that were collected in situ by probes were not included. The reasons for excluding RCM data, are ongoing investigations showing a high sensitivity of the RCM design on the measured data (e.g. [16, 17]), resulting in highly spread data for the same conditions from different devices. The reasons for excluding the data from the low pressure flames are ongoing studies on the impact of the probe on the flow and temperature field of the flames and consequently on the measured species profiles [18, 19]. In general, these two types of experiments offer very useful insights into chemical kinetics. But for their implementation into optimisation processes, further investigations are required to fully understand their uncertainties.

The fuel-air equivalence ratio φ and the range of pressure p of the experiments from ST, FR and JSR are listed in Tables 1 and 2. The targeted flame

Table 1: List of shock tube experiments utilised for optimisation

Fuel (molar)	φ	Bath gas	p / bar	No. of q	Ref.
Shock tube (ST), ignition delay times					
$H_2/CO = 5/95$	1.0	Ar	1–16	23	[20]
$H_2/CO = 5/95$	0.5	N_2	1–19	48	[21]
$H_2/CO = 10/90$	0.5	N_2	1–17	30	[21]
$H_2/CO = 20/80$	0.5	N_2	1–18	24	[21]
$H_2/CO = 26/74$	1.0	Ar ; N_2	2–20	30	[22]
$H_2/CO = 33/67$	1.0	Ar	2–20	28	[22]
$H_2/CO = 50/50$	1.0	Ar	1–16	20	[20]
$H_2/CO = 50/50$	1.0	Ar ; CO_2	2–20	30	[22]
$H_2/CO = 70/30$	1.0	Ar	2–20	35	[22]
CH_3OH	1.0	Ar	1–16	15	[23]
CH_4	0.5	Ar	1–8	6	[24]
CH_4	2.0	N_2 ; CO_2	1–10	35	[25]
CH_4	2.0	Ar ; CO_2	1	6	[26]
C_2H_2	0.5 ; 1.0	Ar	1	33	[27]
C_2H_2	0.5–2.0	N_2 ; Ar	10–30	38	[28]
C_2H_4	1.0	Ar	1	8	[29]
C_2H_6	0.5 ; 1.0	Ar	1	17	[30]
Shock tube (ST), OH and CH* profiles*					
CH_4	0.5 ; 1.0	Ar	1–16	242	[31]
RG = $CH_4/C_2H_6 = 92/8$	1.0	Ar	1–16	189	[32]
H_2/RG = 40/60	0.5 ; 1.0	Ar	1–16	540	[32]
H_2/RG = 80/20	0.5 ; 1.0	Ar	1–16	454	[32]
CO/RG/CO_2 = 25.3/11.4/63.3	1.0	Ar	16	30	[33]
CO/RG/CO_2 = 61.9/5.6/32.5	1.0	Ar	16	33	[33]
$H_2/CO/CH_4/CO_2 = 5/31/38/26$	0.5 ; 1.0	Ar	4	330	[31]

speed measurements are listed in Table 3. Additionally combustion experiments of C_2H_2, C_2H_4 and C_2H_6 were added to the experimental data set. These components are important intermediates for the fuel rich combustion of methane and at the same time are typical minor components of natural gas, relevant for various applied combustion systems.

The ignition delay times were defined by measurements of photon emissions from excited OH or CH radicals. Thereby, they were defined by the maximum emission (e.g. [20]) or by the intersection method (e.g. [29]). If

Table 2: List of flow reactor, jet stirred reactor and burner stabilised flame experiments utilised for optimisation

Fuel (molar)	φ	Bath gas	p / bar	No. of q	Ref.
Flow reactor (FR)					
H_2	0.3–1.0	N_2	0.3–16	28	[34]
CO	1.0	N_2 ; H_2O	3.5 ; 9.7	6	[35]
CH_2O	1/225–1/150	N_2 ; H_2O	1.5 ; 9.7	24	[36]
CH_4	0.5 ; 1.0 ; 2.0	Ar	1	33	[37]
CH_4	0.06 ; 1.0 ; 19.7	N_2	100	35	[38]
C_2H_2	1.0 ; 1.4	N_2	1	28	[39]
C_2H_4	0.5 ; 1.0	Ar	1	34	[37]
C_2H_4	2.5	N_2	5 ; 10	33	[40]
Jet stirred reactor (JSR)					
H_2	0.2	N_2	1	4	[5]
H_2/CO = 50/50	0.2	N_2	1	6	[41]
CH_3OH	0.5–2.0	N_2	1–20.3	80	[42]
CH_4	0.1	N_2	1	20	[5]
CH_4	0.1 ; 0.5 ; 1.0	N_2	1 ; 10	50	[43]
CH_4	1.5	N_2	10	18	[44]
H_2/CH_4 = 50/50	0.3	N_2 ; CO_2	1 ; 10	71	[5]
H_2/CH_4 = 50/50	1.0 ; 1.5	N_2 ; CO_2	1 ; 10	61	[44]
H_2/CO/CH_4 = 25/25/50	0.3	N_2	1	24	[5]
H_2/CO/CH_4 = 25/25/50	1.5	N_2	1	18	[44]
C_2H_2	0.4 ; 1.0	N_2	1	53	[45]
Burner stabilised flame (BF)					
CH_4	1.0–1.9	N_2	0.039	26	[46, 47]

available the complete normalised emission profiles of OH and CH chemiluminescence from ST were selected as targets for the optimisation as shown in previous work [15]. The pressure profiles of the ST were taken as input values for the simulation. If these were not available we considered constant pressure until ignition occurs in the ST [31, 32]. More details on the selected pressure conditions are given in the Supplementary Materials. For the FR and JSR the reactants, products and intermediates (CO, CH_2O, C_2H_2, C_2H_4, C_2H_6) were targeted in the optimisation process. For the BF the intermediates HCO and singlet methylene $^1CH_2$ were targeted, which were

Table 3: List of laminar flame speeds utilised for optimisation

Fuel (molar)	T_0 / K	p / atm	Ref.
H_2	298	1	[48]
H_2	298	1	[49]
H_2/N_2 = 30/70	298	1	[50]
H_2/N_2 = 25/75	298	1	[50]
H_2/N_2 = 25/75	298	1	[51]
H_2/CO = 50/50	298	1	[48]
H_2/CO = 50/50	298	2	[52]
H_2/CO/N_2 = 20/20/60	302	1	[53]
H_2/CO/N_2 = 10/20/70	298	1	[50]
H_2/CO/N_2 = 15/15/70	298	1	[50]
H_2/CO/N_2 = 20/10/70	298	1	[53]
H_2/CO/N_2 = 24/6/70	298	1	[50]
H_2/CO/CO_2 = 12/48/40	300	1	[54]
H_2/CO/CO_2 = 30/30/40	300	1	[54]
H_2/CO/CO_2 = 5/45/50	298	1	[55]
H_2/CO/CO_2 = 10/40/50	303	1	[54]
H_2/CO/CO_2 = 25/25/50	303	1	[54]
H_2/CO/CO_2 = 40/10/50	303	1	[54]
CH_3OH	298	1	[56]
CH_3OH	338	1	[56]
CH_4	342	0.1 ; 0.25	[8]
CH_4[a]	298	1	[57]
CH_4	298	1 ; 2 ; 4	[58]
CH_4	358	1	[6]
H_2/CH_4 = 30/70	298	1	[59]
H_2/CH_4 = 35/65	298	1	[60]
H_2/CH_4 = 35/65	298	1	[61]
H_2/CH_4 = 40/60	298	1	[59]
H_2/CH_4 = 50/50	298	1	[60]
H_2/CH_4 = 80/20	303	1	[62]
biogenic mix 1[b]	298	1	[6]
biogenic mix 2[c]	298	1	[6]
C_2H_2	298	1	[63]
C_2H_4	298	1	[63]
C_2H_6	298	1	[63]
$H_2/CH_4/C_2H_6$ = 35/52/13	298	1	[60]

[a] with argon in oxidiser

[b] H_2/CO/CH_4/CO_2/N_2 = 12/19/5.8/13.2/50

[c] H_2/CO/CH_4/CO_2/N_2 = 9.6/15.2/24.6/10.6/40

experimentally measured by the non-intrusive method of intracavity laser spectroscopy (ICLAS). To simulate the in-house FR experiment [37], updated temperature profiles of this FR [64] were used. The selected laminar flame speeds are all derived from stretch corrected burning velocities from counter flow burners, heat flux burners and outwardly propagating flames. In this regard we sustained a low number of flame speed data derived from outwardly propagating flames, due to their higher uncertainties [65]. In total the number n of quantities q targeted by the optimisation is 3011.

Furthermore, the target values were weighted. The targets from the shock tube experiments were weighted by a factor of 1.0 because they are the majority in the target set. The weighting factor was decreased to 0.5 for ignition delay times from shock tubes higher then 1 ms, when no informations on the pressure profile during the experiment were available, due to the increased uncertainty [66]. The other weightings were increased due to their lower uncertainties. Thereby, weighting factors for temperature targets of jet stirred reactors and flow reactors were set to 10.0 because of the low relative uncertainty of the temperature. The weighting for the laminar burning velocities were set to 8.0, except for the burning velocities from outwardly propagating flames. Their weighting factors were halved to a value of 4.0 due to their higher uncertainty.

4. Chemical Kinetic Model

To create a base chemical kinetic model for the optimisation, the in-house model DLR-RG [3] was selected as the baseline model. The model was extended with a sub model for C_3 species from the USC II mechanism [2],

which was required to simulate the C_2 oxidation – especially the laminar flame speeds. For the C_2H_2 oxidation vinylidene was added as an intermediate as suggested by Laskin and Wang [67]. As another major update for the simulation of the C_2H_2 oxidation – mainly of the JSR experiments – the multi channel reactions of triplet methylene radical and the vinyl radical with molecular oxygen needed to be updated:

$$\begin{aligned} {}^3CH_2 + O_2 &\rightleftharpoons CO_2 + H_2, && \text{(R1a)} \\ &\rightleftharpoons CO_2 + H + H && \text{(R1b)} \\ &\rightleftharpoons CO + H_2O && \text{(R1c)} \\ &\rightleftharpoons CO + OH + H && \text{(R1d)} \\ &\rightleftharpoons CH_2O + O && \text{(R1e)} \end{aligned}$$

$$\begin{aligned} C_2H_3 + O_2 &\rightleftharpoons CO_2 + CH_3 && \text{(R2a)} \\ &\rightleftharpoons CO + CH_3O && \text{(R2b)} \\ &\rightleftharpoons CH_2O + HCO && \text{(R2c)} \\ &\rightleftharpoons C_2H_2 + HO_2 && \text{(R2d)} \\ &\rightleftharpoons CH_2CHOO && \text{(R2e)} \\ &\rightleftharpoons CH_2CHO + O && \text{(R2f)} \\ &\rightleftharpoons CH_2CO + OH && \text{(R2g)} \\ &\rightleftharpoons CHCHO + OH && \text{(R2h)} \\ &\rightleftharpoons CHOCHO + H && \text{(R2i)} \end{aligned}$$

Thereby, the total reaction rate of R1 was taken from Lee et al. [68], which is in very good agreement with the experimental values of Vinkier and Debruyn

[69]. The branching ratios of R1 were updated to the values of Blitz et al. [70] as suggested by Smith et al. [71]. The reaction rates of R2 were taken from the recent quantum chemical study of Goldsmith et al. [72].

The study on the low pressure CH_4 flames [8] showed a strong influence of HCO dissociation due to its weakly bound H atom, as mentioned before. Therefore, partial decomposition of HCO formed was considered in the mechanism as suggested by Labbe et al. [7]. Additionally, submodels for excited OH and CH radicals – required for the ST data – were added as done before in prior work [15, 73, 74].

The thermodynamic data for heat capacities, enthalpies and entropies where updated to recent values of the Active Thermochemical Tables Thermochemical Network (ATcT TN) [75]. In this regard, we implemented ATcT TN version 1.122b, which was taken from Glarborg et al. [76].

For a first sensitivity analysis with the linTM the uncertainties of the rate coefficients were set globally to $\Delta \lg(k) = 0.5$, to identify the most sensitive reactions. For the most sensitive reactions, the rate coefficients and their uncertainties were updated from literature values – mainly from Baulch et al. [9], but also other references [10, 13, 40, 45, 68, 70, 72, 77–90].

For the optimisation of the mechanism the rate coefficients were constrained within their 3σ uncertainty range. 89 reactions were optimised with a total of 475 parameters, which are mainly the Arrhenius parameters of the rate coefficients. Parameters were only optimised if one of their sensitivity $S_{r,j}$ for any characteristic point j was at least 5% of the maximum sensitivity for this specific characteristic point j. With this restriction, parameters are only optimised that are relevant to the set of targeted data. The opti-

mised mechanism and the base values of the optimised parameters including their uncertainties are given as Supplementary Materials. As a benchmark the optimised chemical kinetic model is compared to established conventional models: POLIMI C1-C3 v1412 [91], FFCM 1.0 [71], USC mech 2.0 [2], Aramco 2.0 [92], a recent model by Glarborg et al. [76] and the in-house model DLR-RG [3]. For all chemical kinetic simulations the open-source software Cantera was used [93].

5. Results and Discussion

The unweighted average absolute distances $\bar{d}$ between simulation and experiment of the characteristic points for the different experiments and investigated models are summarised in Table 4. With the model adaptations of the model DLR-RG these average distances of the base model are moderately reduced. Hence, the performance of the base model is similar to the recent models, which are shown in Table 4.

With the optimisation within the parameter uncertainties it is possible to significantly increase the model's capability to reproduce the all types of experimental data. For that matter, the overall average distance of all targeted points could be reduced by about a factor of two compared to the other models from literature. And, the results of the optimised model DLR SynNG agree considerably better with all investigated experiment types compared to the other models.

5.1. Laminar Burning Velocities

The simulation results of the laminar flame speeds by the optimised model are in excellent agreement with the experimental burning velocities. Exam-

Table 4: List of average absolute distances $\bar{d}$ of the characteristic points between experiments and simulation results with the different chemical kinetic models.

Model	Species	Reactions[a]	$\bar{d}_{\mathrm{ST}}$	$\bar{d}_{\mathrm{JSR}}$	$\bar{d}_{\mathrm{FR}}$	$\bar{d}_{\mathrm{BF}}$	$\bar{d}_{\mathrm{FS}}$	$\bar{d}_{\mathrm{overall}}$
		$n =$	2243	405	221	26	116	3011
POLIMI v1412	107	2642	0.308	0.066	0.274	0.313	0.055	0.264
FFCM 1.0	38	291	0.263	0.062	0.576	0.171	0.043	0.250
USC 2.0	111	784	0.221	0.097	0.374	0.144	0.047	0.209
Aramco 2.0	493	2716	0.222	0.045	0.262	0.190	0.044	0.194
Glarborg 2018	151	1393	0.226	0.050	0.190	0.121	0.039	0.192
DLR-RG	65	395	0.267	0.162	0.378	0.598	0.044	0.256
Base model	83	747	0.181	0.087	0.353	0.126	0.050	0.176
DLR-SynNG (optimised, this work)	83	747	0.107	0.031	0.107	0.063	0.035	0.094

[a] As counted by Cantera [93]

ples of these comparisons are given in Figures 1–4. Figure 1 shows that the optimised model can predict pure hydrogen and syngas mixtures burning velocities as well as the conventional models. The burning velocities are in very good agreement with the experimental values from the heat flux burner in Figure 1 (b) and (c) and slightly underpredict the burning velocities of the bomb measurements in Figure 1 (a). The reason for the deviation between numerical and experimental results of the bomb experiments can be related to the higher experimental uncertainties of this experiment. These uncertainties are also reflected in the lower weighting for these experimental targets in this optimisation, as mentioned before. Further comparisons are detailed in the Supplementary Materials.

The optimised model also agrees well with measured laminar flame speeds for pure methane for a wide pressure range as shown in Fig. 2. Due to the implementation of the partial dissociation of the weakly bound HCO radical in the chemical kinetic model, the simulated low pressure flame speeds are

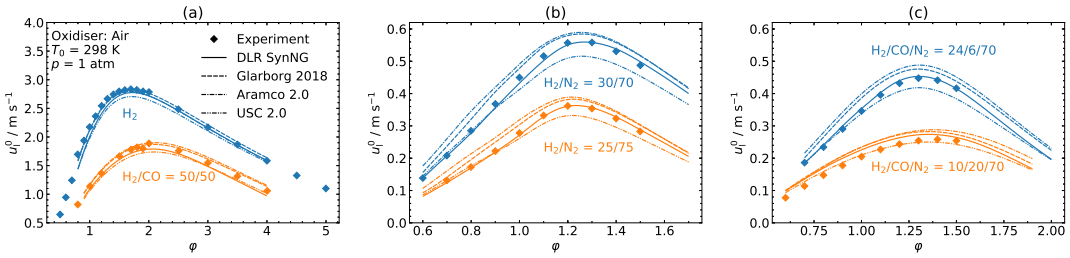

Figure 1: Simulation results of laminar flames speeds of H_2, CO and their mixtures compared to experimental data from Krejci et al. [48] (a) and Voss et al. [50] (b) and (c)

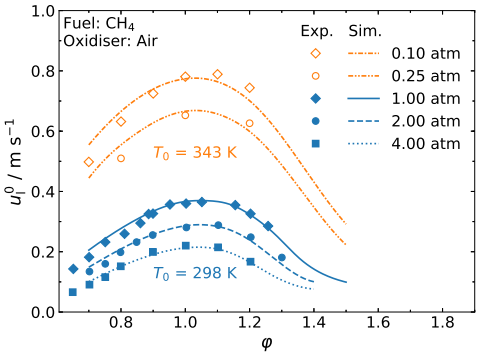

Figure 2: Simulation results of laminar flame speed simulations of methane by the optimised chemical kinetic model compared to experiments from Burrell [8] for sub atmospheric and from Park et al. [58] for atmospheric and elevated pressure

in good agreement with the experimental results [8]. The described pressure range in Fig. 2 is relevant for decentralised power generation from natural gas or biogenic gas mixtures at slightly elevated pressure in micro gas turbine combustion or at subatmospheric pressure e.g. for the inverted Brayton cycle [94].

All compared models agree well with pure syngas mixtures and pure methane burning velocities. Contrary, as shown in Figure 3 none of the con-

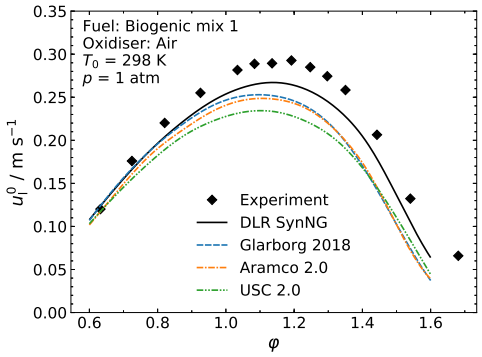

Figure 3: Simulation results of laminar flames speeds of biogenic mix I (H_2/CO/CH_4/CO_2/N_2 = 12/19/5.8/13.2/50) compared to experimental data from Yan et al. [6]

ventional models is capable to reproduce the laminar burning velocities of the mixed syngas methane fuel or biogenic fuel mix, respectively. Thus, only the optimised model is able to consistently reproduce the laminar burning velocities of syngas and methane as well as their mixtures.

For the simulation of combustion processes with natural gas, accurate modelling of the kinetics of the C_2 species is required. In this regard, also the burning velocities for the C_2 species are consistently reproduced by the optimised model (Figure 4). Thereby, Figure 4 (a) illustrates a significant increase in accuracy predicting the experimental data for the ethane combustion from Park et al. [63].

5.2. Ignition Delay Times

The average distances of the targeted shock tube data $\bar{d}_{\mathrm{ST}}$ is decreased by around a factor of two compared to the conventional models. The average distances by the optimised model are considerably small compared to general

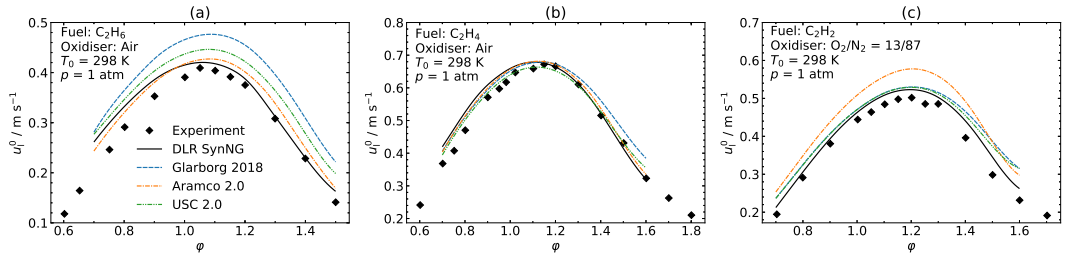

Figure 4: Simulation results of laminar flame speed simulations of C_2 fuels compared to experiments from Park et al. [63]

assumption of approximately 15% standard deviation of the statistical error of shock tube measurements – mainly caused by the temperature estimation of the initial temperature behind reflected shock waves [66]. But in this study, mainly shock tube experiments with known temporal pressure profiles have been implemented into the optimisation process, for which studies have indicated a significantly smaller statistical error [65], which is also confirmed by this work.

Measured ignition delay times are well and consistently reproduced for a large pressure range for all investigated fuels. This is exemplary shown for syngas and methane and their mixtures in Fig. 5 and for ethane, ethylene and acetylene in Fig. 6.

Figure 5 (a) illustrates that reproducibility of the ignition delay times of the syngas mixture at high pressures is significantly increased by the optimised model compared to the conventional models. Similar observations of increasing reproducibility can be demonstrated for the ignition delay times of the C_2 species in Fig. 6. The whole model performance on the ignition delay times is shown in the Supplementary Materials.

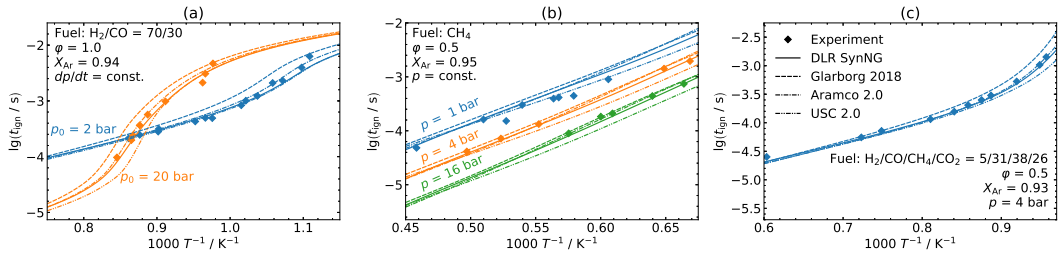

Figure 5: Simulation results of ignition delay times of syngas, CH_4 and their mixture compared to experimental data from Thi et al. [22] (a) and Herzler et al. [31] (b) and (c)

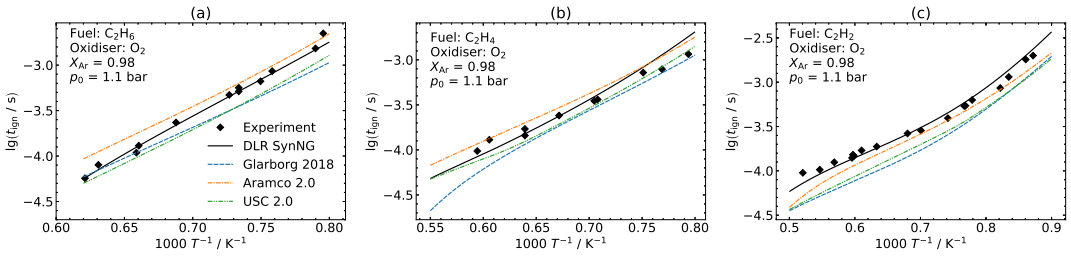

Figure 6: Simulation results of ignition delay times of syngas, CH_4 and their mixture compared to experimental data from Vries et al. [30] (a), Petersen et al. [29] (b) and Rickard et al. [27] (c)

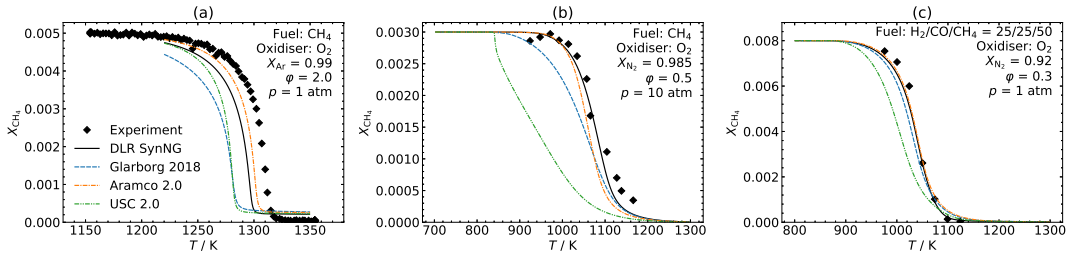

Figure 7: Simulation results of CH_4 profiles from the oxidation of CH_4 and its mixture with syngas compared to experimental FR data from Oßwald et al. [37] (a) and JSR data from Dagaut et al. [5] (b) and (c)

5.3. Species Profiles

Figure 7 shows that the low temperature oxidations of CH_4 in the FR (a) and the JSR (b) and (c) are in good agreement with the optimised model. Contrary, the model USC 2.0 overestimate the consumption of CH_4 at lower temperatures for both independent experiment types. Firstly, the optimisation with the linTM is successfully applied to data from the JSR, which is demonstrated further by the exemplary results of the intermediate C_2H_4 from the combustion of CH_4 and mixtures with syngas (Fig. 8). To wit, the simulated C_2H_4 profiles of the optimised model are in very good agreement for atmospheric pressure (a) and (c) and at elevated pressure (b). Thereby, the maximum concentration as well as the time scales of production and consumption of C_2H_4 are accurately reproduced.

Figures 9 and 10 show that the oxidation of C_2H_4 and C_2H_2 are also well reproduced with the optimised model. Contrary, all conventional model overestimate the consumption of C_2H_4 in the FR and C_2H_2 in the JSR. Also, the time scales and the maximum concentration of the intermediate CH_4 are in

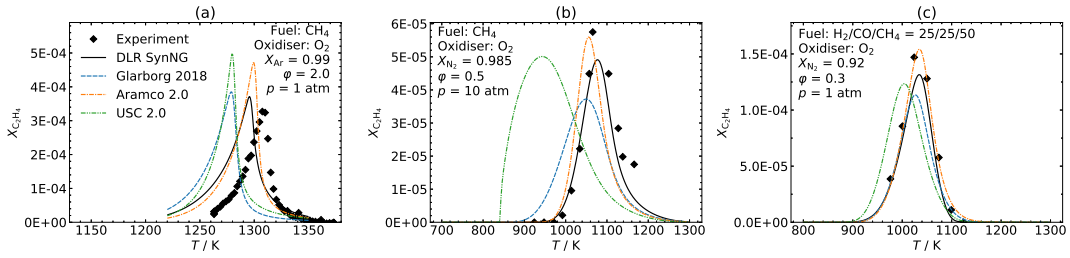

Figure 8: Simulation results of C_2H_4 profiles from the oxidation of CH_4 and its mixture with syngas compared to experimental FR data from Oßwald et al. [37] (a) and JSR data from Dagaut et al. [5] (b) and (c)

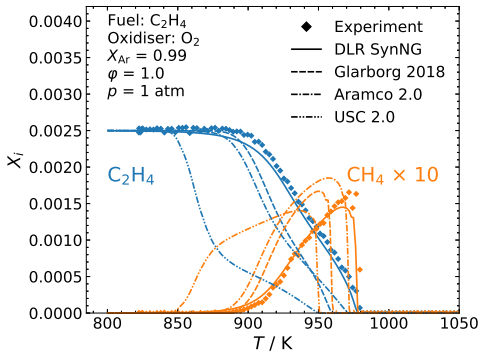

Figure 9: Simulation results of C_2H_4 and CH_4 profiles from the oxidation of C_2H_4 compared to experimental FR data from Oßwald et al. [37]

very good agreement with the optimised model. Especially the reproducibility of the experimental data of CH_4 in the JSR can be significantly increased compared to the conventional models.

Also the experimental and numerical species profiles of the burner stabilised flame (BF) are in good agreement (Fig.11). All models are in good agreement with the peak concentration of singlet methylene $^1CH_2$ for the stoichiometric case, with the exception of the model USC 2.0. In contrast,

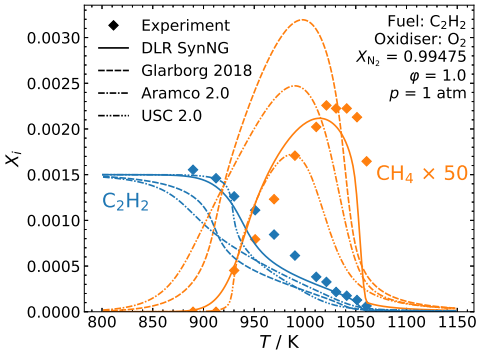

Figure 10: Simulation results of C_2H_2 and CH_4 profiles from the oxidation of C_2H_2 compared to experimental JSR data from Tan et al. [45]

only the optimised model is able to reproduce the experimental data at rich conditions.

In general the capability of optimised model to reproduce the species profiles is one of its major advantages compared to the conventional models considered in this study. Especially the formation of intermediate hydrocarbons is essential for the formation of prompt NO. Thereby, the optimised model with an addition of a NO submodel could have an eminent impact on the accurate simulation of oxidation processes in combustion machinery, and therefore, being crucial for the design of low pollutant applications. Additionally, a significant increase in reproducibility was observed for the toxic intermediate CH_2O (see Supplementary Materials), which is also important for the design of low pollutant combustion, particularly when oxygenated hydrocarbon fuels are burnt [95].

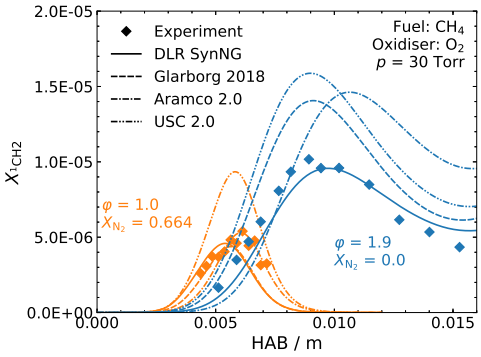

Figure 11: Simulation results of $^1CH_2$ profiles from the oxidation of CH_4 compared to experimental BF data from Fomin et al. [47]

5.4. Optimised Chemical Kinetic Model

The global sensitivity coefficients S_r as defined in Eq. (3) for the reaction rates of the base model k_0 and the optimised model k_{opt} are given in Fig. 12. For the linTM these sensitivities are normalised with their maximum uncertainty. The trend for most S_r of the reactions does not change significantly, demonstrating the robustness of this definition of the global sensitivity. There are also exceptions to that, which will be discussed later in this section.

A profound uncertainty estimation of the model parameters – or rate coefficients, respectively – is challenging and almost impractical from these kinds of optimisation approaches. The main reasons are: (a) Due to the high number of model parameters in chemical kinetic models for the investigated combustion processes, systematic errors – e.g. not yet discovered important pathways or significant under- or overestimations of rate coefficients – cannot be fully excluded; (b) also systematic errors from experiments cannot be fully

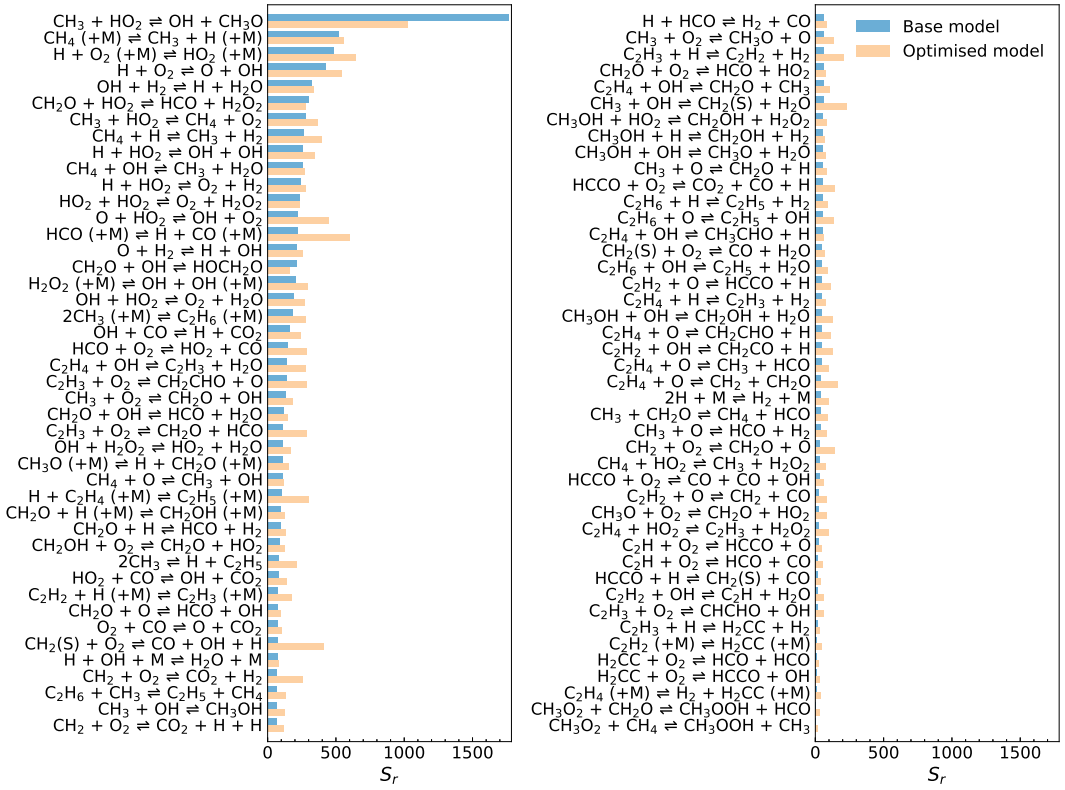

Figure 12: Results of the global sensitivity analysis of the optimised reactions before and after the optimisation

Table 5: Reaction rate coefficients of the 20 most sensitive reactions before and after optimisation

	Base model					*Optimised model*		
Reaction	A	b	E_A	$\Delta \lg(k)_\mathrm{max}$	Ref.	A	b	E_A
$CH_3+HO_2 \rightleftharpoons OH+CH_3O$	1.81e+13	0.00	0.0	1.00	[9]	1.37e+18	-1.81	-2225.8
CH_4 (+M) $\rightleftharpoons CH_3+H$ (+M)	6.41e+17	-0.00	89812.0	0.50	[86]	6.76e+06	3.35	88926.4
$H+O_2$ (+M) $\rightleftharpoons HO_2$ (+M)	1.74e+19	-1.23	0.0	0.20	[78]	1.46e+19	-1.22	0.0
$H+O_2 \rightleftharpoons O+OH$	1.04e+14	0.00	15286.0	0.07	[77]	5.01e+12	0.33	13622.8
$OH+H_2 \rightleftharpoons H+H_2O$	2.16e+08	1.52	3430.0	0.30	[9]	9.14e+06	1.91	2995.7
$CH_2O+HO_2 \rightleftharpoons HCO+H_2O_2$	1.00e+12	0.00	8000.0	0.50	[3]	7.28e-09	6.03	-21.3
$CH_3+HO_2 \rightleftharpoons CH_4+O_2$	1.16e+05	2.23	-3022.0	0.50	[83]	1.11e+19	-1.97	2298.5
$CH_4+H \rightleftharpoons CH_3+H_2$	6.14e+05	2.50	9581.9	0.40	[9]	3.50e+02	3.48	7486.9
$H+HO_2 \rightleftharpoons OH+OH$	5.79e+13	0.00	170.9	0.20	[13]	7.30e+01	3.76	-3301.9
$CH_4+OH \rightleftharpoons CH_3+H_2O$	1.37e+06	2.18	2680.9	0.30	[9]	3.81e+13	-0.09	4956.9
$H+HO_2 \rightleftharpoons O_2+H_2$	2.12e+06	2.11	-1623.8	0.30	[13]	1.65e+02	3.16	-6376.0
$HO_2+HO_2 \rightleftharpoons O_2+H_2O_2$	4.22e+14	0.00	11974.8	0.40	[9]	1.16e+21	-1.94	14798.4
$O+HO_2 \rightleftharpoons OH+O_2$	1.63e+13	0.00	-444.8	0.50	[9]	1.71e+06	2.47	-1692.7
HCO (+M) $\rightleftharpoons H+CO$ (+M)	4.94e+10	0.96	14631.8	0.30	[13]	1.24e+43	-8.37	33089.7
$O+H_2 \rightleftharpoons H+OH$	3.83e+12	0.00	7943.5	0.20	[9]	1.94e+15	-0.80	8746.1
$CH_2O+OH \rightleftharpoons HOCH_2O$	4.50e+15	-1.10	0.0	0.50	[3]	9.77e+14	-1.13	0.0
H_2O_2 (+M) $\rightleftharpoons OH+OH$ (+M)	1.20e+17	0.00	45476.6	0.20	[9]	1.22e-12	8.59	31740.3
$OH+HO_2 \rightleftharpoons O_2+H_2O$	9.58e+11	0.42	-948.1	0.20	[13]	4.66e+09	1.06	-2811.4
$2CH_3$ (+M) $\rightleftharpoons C_2H_6$ (+M)	1.27e+41	-7.00	2760.4	0.30	[9]	3.13e+47	-8.68	6435.5
$OH+CO \rightleftharpoons H+CO_2$	2.23e+05	1.90	-1160.0	0.20	[36]	1.90e+05	1.91	-1211.7

Units: A: cm, mol, s; E_A: cal mol^{-1}

[a] Low pressure values of fall-off reaction

neglected. Consequently, uncertainty quantification results can be highly influenced by systematic errors. Therefore, resulting rate coefficients and their uncertainties estimations from these optimisation approaches should not be seen as physically granted parameter boundaries and can otherwise be misleading for chemical kinetic modelling. Hence, implementing these results into other models needs to be done thoroughly with diligent validation. Nevertheless, valuable information from these optimisation approaches can still be gained for sensitive reactions, to give leads towards further investigations for certain reactions. For this purpose, we define a local solution space λ_Δ that is defined by the solutions for which the objective function satisfies:

$$\lambda_\Delta = F \leq \sum_{j=1}^{D} (w_j d_{\mathrm{opt},j})^2 \, (1+\Delta)^2. \tag{4}$$

In this equation $d_{\mathrm{opt},j}$ are the distances for the optimised model and Δ is an approximated relative increase of the standard deviation of the distances. With the simplified linearity approximation of the linTM, solutions of the objective function can be estimated. This estimation is shown in Fig. 13 (a) and (b) for an exemplary reaction with its model parameters $\Delta \lg(k(T_1))$, $\Delta \lg(k(T_1))$ and ΔE_A (which define the reaction rate coefficient $k(T)$ and are also shown in Fig. 14). Combinations of input parameters that fulfil Eq. (4) can be found analytically, which are also plotted in Fig. 13 for $\lambda_{0.2}$. In the solution space of the three model parameters of the reaction rate coefficient in Fig. 13 (c), the solution space λ_Δ becomes an angled ellipsoid. The parameter combinations fulfilling $\lambda_{0.2}$ from Fig. 13 (c) can then be projected to the corresponding boundaries of the optimised rate coefficient $k_{\mathrm{opt}}(T)$ in Fig. 14.

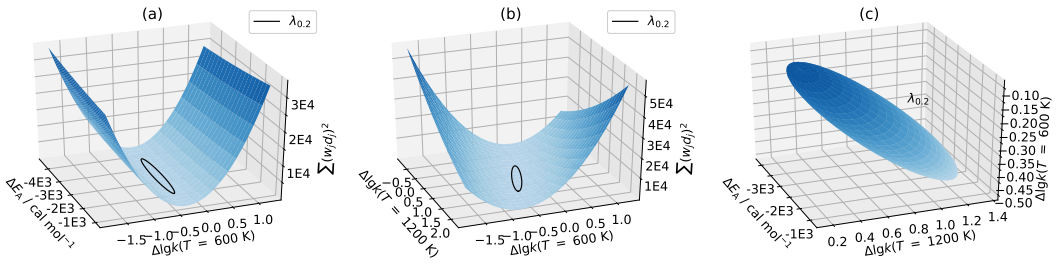

Figure 13: Estimation of the objective function with the deviation of the model parameters of reaction CH_3+HO_2 ⇌CH_3O+OH (a) and (b) and the corresponding local solution space λ_Δ formed by the model parameter (c)

Figures 14 and 15 show the results of the local solution space investigations of the reactions:

$$\mathrm{CH_3 + HO_2 \rightleftharpoons CH_3O + OH,} \tag{R3a}$$

$$\rightleftharpoons \mathrm{CH_4 + O_2,,} \tag{R3b}$$

for which R3a is the most sensitive reaction of this optimisation problem. Figure 14 illustrates that the local solution space λ_Δ of $k(T)$ of R3a becomes significantly small around temperatures of about 1000 K. In this temperature range, the optimised $k_{\mathrm{opt}}(T)$ is in excellent agreement with and supported by the experimental estimation of Scire et al. [96] and the review value of Baulch et al. [9] – here the base rate coefficient k_0. The optimised value of the E_A of R3a is -2.225 cal/mol. Negative temperature dependencies can be found for various reactions and are implemented in any modern detailed chemical kinetic model. Reasons are for instance temperature dependencies of activation energies, which not necessarily have to be constant. Also more complex reaction phenomena cannot be fully displayed by the highly simplified theory behind the semi-empirical Arrhenius equation, for which the

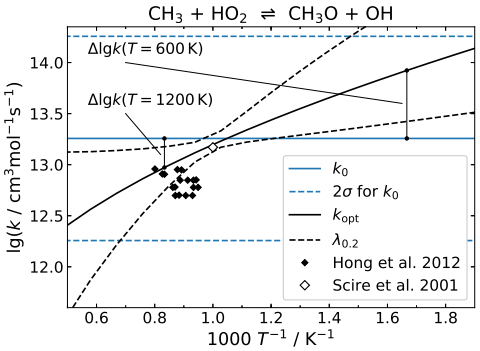

Figure 14: Optimised rate coefficient of reaction R3a with the base model k_0 from Baulch et al. [9] and experimental results from Scire et al. [96] and Hong et al. [97]

Arrhenius parameter become pure fitting parameters (e.g. [72]). A negative E_A for reaction R3a was also reported by quantum chemical calculations [83]. Furthermore, with the negative E_A, the model even agrees well with the the upper values of highly scattered experimental estimation of R3a by shock tube experiments from Hong et al. [97], supporting the optimised result.

Figure 15 illustrates that channel R3b agrees very well with experimental results from Hong et al. [97] and Scire et al. [96] and quantum chemical modelling results from Jasper et al. [83] (here k_0) around the temperature range of 1000–1200 K. For higher temperatures the values of the optimised value k_{opt} and the base model value k_0 from Jasper et al. [83] show different trends and diverge. Srinivasan et al. [98] studied the reverse reaction of R3b experimentally. The corresponding values from reversing their results are also shown in Fig. 15 and their highly scattered data agree with both rate coefficients k_{opt} and k_0. Thus, for final conclusions on the rate coefficient value of R3b at higher temperatures more investigations are required.

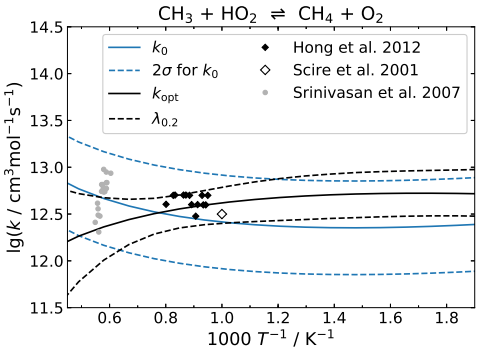

Figure 15: Optimised rate coefficient of reaction R3b with the base model k_0 from Jasper et al. [83] and experimental results from Scire et al. [96], Srinivasan et al. [98] and Hong et al. [97]

Another sensitive reaction that has been studied intensively by experiments is:

$$\mathrm{CH_4(+M) \rightleftharpoons CH_3 + H(+M)}, \tag{R4}$$

for which the optimisation results are shown in Fig. 16. Even though the experimental values of Davidson et al. [99] were not directly targeted by the optimisation, the optimised rate coefficient k_{opt} is in outstanding good agreement with the experimental data. Also the trend of k_{opt} agrees well with the experimental data of Wang et al. [86], which were experimentally determined in a shock tube study at lower temperature. Therefore, deviations can be associated with higher uncertainties of shock tube results regarding low temperatures [66].

In general, there is a very good agreement of the presented, sensitive rate coefficients with the independent experimental determinations. This indicates a potentially low impact of a systematic error on the optimisation

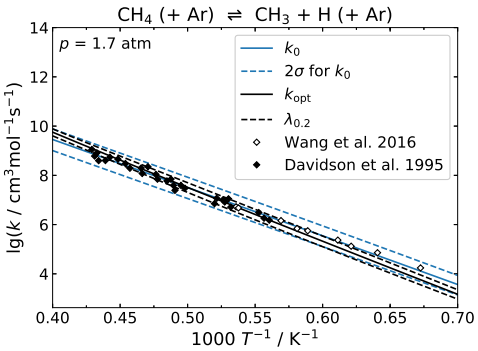

Figure 16: Optimised rate coefficient of reaction R4 with the base model k_0 from Wang et al. [86] and experimental results from Wang et al. [86] and Davidson et al. [99]

results of this work.

A reaction that significantly increased its global sensitivity coefficient S_r after the optimisation is the reaction of singlet methylene with molecular oxygen:

$$^1CH_2 + O_2 \rightleftharpoons CO + OH + H. \tag{R5a}$$

Figure 17 shows that the value k_{opt} is pushed to the upper boundary of 3σ after the optimisation process. Since R5 is a chain branching reaction, the increased value has a high impact on the combustion processes investigated in this study, therefore, leading to the increased S_r. There have been a few experimental investigations on reaction R5a with contrary results. On the one hand Shaub et al. [100] concluded, that R5a was the main channel for the reaction of $^1CH_2$ with O_2, which was applied to the direct measurement of the overall rate of the reaction of $^1CH_2$ with O_2 by Langford et al. [101]. In contrast experiments by Hancock et al. [102] indicated that the main channel for this reaction was the deactivation of singlet methylene to triplet

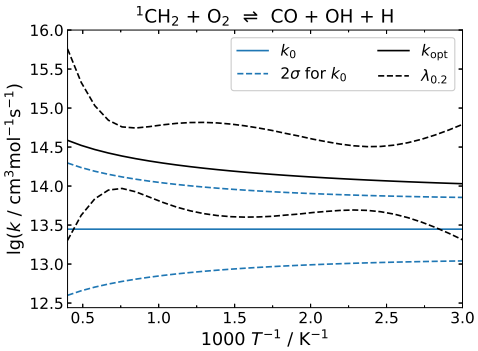

Figure 17: Optimised rate coefficient of reaction R5 with the base model k_0 from Langford et al. [101]

methylene, for which O_2 just acts as a third body:

$$^1CH_2 + O_2 \rightleftharpoons {}^3CH_2 + O_2. \tag{R5b}$$

But also with the indications of Hancock et al. [102] no final conclusion on the reaction of $^1CH_2$ with O_2 can be drawn.

The incorporation of reaction R5 is consequently inconclusive among recent chemical kinetic models. For instance is the value suggested by Langford et al. [101] is incorporated in the models like GRI 3.0 [1], USC 2.0 [2] or Aramco 2.0 [92], but this reaction is completely left out in the model of Glarborg et al. [76]. The possible importance of reaction R5 in the optimised model underlines the need of further investigations on the rate coefficient of this reaction, e.g., by quantum chemical simulations of the reaction.

6. Conclusions

Within this work an optimised chemical kinetic model was established, which can reproduce fundamental experimental data from the oxidation of

fuel mixtures of H_2, CO, CH_4 and C_2 species with high accuracy. The average deviation between experimental and simulated targets can be reduced by a factor of two compared to conventional models. The optimised model can consistently reproduce data from shock tubes, flow reactors, jet stirred reactors and different burner types. Here, the reproduction of low temperature combustion in flow reactors and jet stirred reactors could be significantly improved. Also the laminar flame speeds of mixtures of syngas and methane are reproduced more accurately compared to the conventional models. The combustion model is valid for a wide range of boundary conditions, relevant for applied combustion systems, e.g., for power generation from biogenic gases in decentralised units. Due to the implementation of partial dissociation of the weakly bound HCO radical, the model is also capable to accurately reproduce data at subatmospheric conditions.

Thus, the optimised combustion model is capable of reproducing relevant combustion characteristics for the design of combustion machinery, like the ignition behaviour, the heat release and intermediate species. Whereas ignition behaviour and heat release are important for the reliability (e.g. flashback risk) and the dimensioning of combustion chambers, heat release and intermediates are also important for the prediction of pollutant emissions. Thereby, intermediates can directly be pollutants. Additionally, when adding NO_x models, heat release is important for the accurate modelling of thermal NO_x and the accurate modelling of hydrocarbon intermediates is important for the prediction of prompt NO.

Therefore, the chemical kinetic model can be used for the numerical design or adaptation of combustion chambers, e.g., by CFD simulations, to

guarantee reliable operation of combustion machinery at low pollutant emission levels. In this context the chemical kinetic model can also serve as a base model for the generation of numerically efficient reduced models.

With the analysis of the chemical kinetic model, the reaction of singlet methylene with molecular oxygen was identified as a key reaction in the optimised model. For this reaction further investigations seem to be of high interest, e.g., by quantum chemical modelling approaches. For the further chemical kinetic evaluation of the rate coefficients more experimental data could be collected and implemented into the overall optimisation process. As examples species profiles probed from flat laminar flames and combustion data from rapid compression machines could be implemented. Also, chemical kinetic submodels for NO_x could be added to the model and included directly in the optimisation process.

On the whole, the optimisation method, utilised in this work, is very general. This optimisation work can be extended and the method can be used on arbitrary reaction schemes for a broad variety of fuels in different fundamental experiments.

Acknowledgments

The support by the Helmholtz-Gemeinschaft within the project DLR@Uni (Grant No. HA-302) is thankfully acknowledged.

Supplementary Materials

The optimised chemical kinetic model as well as a full illustration of the model's perfomrance on the targeted experimental data are available as

Supplementary Materials.

References

[1] G. P. Smith, D. M. Golden, M. Frenklach, N. W. Moriarty, B. Eiteneer, M. Goldenberg, C. T. Bowman, R. K. Hanson, S. Song, W. C. Gardiner Jr., V. V. Lissianski, Z. Qin, GRI 3.0 mechanism, `http://combustion.berkeley.edu/gri_mech/` (11 2017).

[2] H. Wang, X. You, A. V. Joshi, S. G. Davis, A. Laskin, F. Egolfopoulos, C. K. Law, USC mech version II. high-temperature combustion reaction model of H2/CO/C1-C4 compounds, `http://ignis.usc.edu/USC_Mech_II.htm` (2007).

[3] M. Braun-Unkhoff, N. Slavinskaya, M. Aigner, A detailed and reduced reaction mechanism of biomass-based syngas fuels, Journal of Engineering for Gas Turbines and Power 132 (9) (2010) 091401.

[4] M. Fischer, X. Jiang, An assessment of chemical kinetics for bio-syngas combustion, Fuel 137 (2014) 293–305.

[5] T. Le Cong, P. Dagaut, G. Dayma, Oxidation of natural gas, natural gas/syngas mixtures, and effect of burnt gas recirculation: Experimental and detailed kinetic modeling, Journal of Engineering for Gas Turbines and Power 130 (4) (2008) 041502.

[6] B. Yan, Y. Wu, C. Liu, J. Yu, B. Li, Z. Li, G. Chen, X. Bai, M. Aldén, A. Konnov, Experimental and modeling study of laminar burning ve-

locity of biomass derived gases/air mixtures, international journal of hydrogen energy 36 (5) (2011) 3769–3777.

[7] N. J. Labbe, R. Sivaramakrishnan, C. F. Goldsmith, Y. Georgievskii, J. A. Miller, S. J. Klippenstein, Weakly bound free radicals in combustion: prompt dissociation of formyl radicals and its effect on laminar flame speeds, The journal of physical chemistry letters 7 (1) (2015) 85–89.

[8] R. R. Burrell, Studies of methane counterflow flames at low pressures, Ph.D. thesis, University of Southern California (2017).

[9] D. L. Baulch, C. T. Bowman, C. J. Cobos, R. Cox, T. Just, J. A. Kerr, M. J. Pilling, D. Stocker, J. Troe, W. Tsang, R. W. Walker, J. Warnatz, Evaluated kinetic data for combustion modeling: Supplement II, J. Phys. Chem. Ref. Data 34 (3) (2005) 757–1397.

[10] S. G. Davis, A. V. Joshi, H. Wang, F. Egolfopoulos, An optimized kinetic model of H_2/CO combustion, Proceedings of the Combustion Institute 30 (1) (2005) 1283–1292.

[11] X. You, T. Russi, A. Packard, M. Frenklach, Optimization of combustion kinetic models on a feasible set, Proceedings of the Combustion Institute 33 (1) (2011) 509–516.

[12] T. Varga, T. Nagy, C. Olm, I. G. Zsély, R. Pálvölgyi, É. Valkó, G. Vincze, M. Cserháti, H. Curran, T. Turányi, Optimization of a hydrogen combustion mechanism using both direct and indirect mea-

surements, Proceedings of the Combustion Institute 35 (1) (2015) 589–596.

[13] T. Varga, C. Olm, T. Nagy, I. G. Zsély, É. Valkó, R. Pálvölgyi, H. J. Curran, T. Turányi, Development of a joint hydrogen and syngas combustion mechanism based on an optimization approach, International Journal of Chemical Kinetics 48 (8) (2016) 407–422.

[14] H. Lee, A. Mohamad, L. Jiang, A detailed chemical kinetics for the combustion of $H_2/CO/CH_4/CO_2$ fuel mixtures, Fuel 193 (2017) 294–307.

[15] T. Methling, M. Braun-Unkhoff, U. Riedel, A novel linear transformation model for the analysis and optimisation of chemical kinetics, Combustion Theory and Modelling 21 (3) (2017) 503–528.

[16] G. Mittal, S. Gupta, Computational assessment of an approach for implementing crevice containment in rapid compression machines, Fuel 102 (2012) 536–544.

[17] K. P. Grogan, S. S. Goldsborough, M. Ihme, Ignition regimes in rapid compression machines, Combustion and Flame 162 (8) (2015) 3071–3080.

[18] A. T. Hartlieb, B. Atakan, K. Kohse-Höinghaus, Effects of a sampling quartz nozzle on the flame structure of a fuel-rich low-pressure propene flame, Combustion and flame 121 (4) (2000) 610–624.

[19] N. Hansen, R. Tranter, J. Randazzo, J. Lockhart, A. Kastengren, Investigation of sampling-probe distorted temperature fields with x-ray flu-

orescence spectroscopy, Proceedings of the Combustion Institute 37 (2) (2019) 1401–1408.

[20] J. Herzler, C. Naumann, P. Griebel, Ignition delay time measurements for the validation of reaction mechanisms for fuels from gasification processes, in: Proceedings of the European Combustion Meeting - 2011, no. 336, European Combustion Meeting, Cardiff, UK, 2011.

[21] D. M. Kalitan, J. D. Mertens, M. W. Crofton, E. L. Petersen, Ignition and oxidation of lean CO/H_2 fuel blends in air, Journal of propulsion and power 23 (6) (2007) 1291–1303.

[22] L. D. Thi, Y. Zhang, Z. Huang, Shock tube study on ignition delay of multi-component syngas mixtures–effect of equivalence ratio, international journal of hydrogen energy 39 (11) (2014) 6034–6043.

[23] J. Herzler, C. Naumann, Ignition delay time measurements for the validation of reaction mechanisms for different alcohols, in: Proceedings of the European Combustion Meeting - 2013, no. P3-8, European Combustion Meeting, Lund, Sweden, 2013.

[24] E. L. Petersen, J. M. Hall, S. D. Smith, J. de Vries, A. R. Amadio, M. W. Crofton, Ignition of lean methane-based fuel blends at gas turbine pressures, Journal of Engineering for Gas Turbines and Power 129 (4) (2007) 937–944.

[25] W. Zeng, H. Ma, Y. Liang, E. Hu, Experimental and modeling study on effects of N_2 and CO_2 on ignition characteristics of methane/air mixture, Journal of advanced research 6 (2) (2015) 189–201.

[26] B. Koroglu, O. M. Pryor, J. Lopez, L. Nash, S. S. Vasu, Shock tube ignition delay times and methane time-histories measurements during excess CO_2 diluted oxy-methane combustion, Combustion and flame 164 (2016) 152–163.

[27] M. Rickard, J. Hall, E. Petersen, Effect of silane addition on acetylene ignition behind reflected shock waves, Proceedings of the Combustion Institute 30 (2) (2005) 1915–1923.

[28] N. Lokachari, U. Burke, A. Ramalingam, M. Turner, R. Hesse, K. P. Somers, J. Beeckmann, K. A. Heufer, E. L. Petersen, H. J. Curran, New experimental insights into acetylene oxidation through novel ignition delay times, laminar burning velocities and chemical kinetic modelling, Proceedings of the Combustion Institute 37 (1) (2019) 583–591.

[29] E. L. Petersen, J. M. Hall, D. M. Kalitan, M. J. Rickard, Ignition delay time measurements of c_2h_x fuels and comparison to several detailed kinetics mechanisms, ASME Paper No. GT2004-GT53926.

[30] J. de Vries, J. M. Hall, S. L. Simmons, M. J. Rickard, D. M. Kalitan, E. L. Petersen, Ethane ignition and oxidation behind reflected shock waves, Combustion and flame 150 (1) (2007) 137–150.

[31] J. Herzler, J. Herbst, T. Kick, C. Naumann, M. Braun-Unkhoff, U. Riedel, Alternative fuels based on biomass: An investigation of combustion properties of product gases, Journal of Engineering for Gas Turbines and Power 135 (3) (2013) 031401.

[32] J. Herzler, C. Naumann, Shock-tube study of the ignition of methane/ethane/hydrogen mixtures with hydrogen contents from 0% to 100% at different pressures, Proceedings of the combustion institute 32 (1) (2009) 213–220.

[33] J. Herzler, C. Naumann, Oxy-fuel ignition delay time measurements for validation of reaction mechanisms, Tech. Rep. D1.4.1003, German Aerospace Center, Institute of Combustion Technology (2010).

[34] M. Mueller, T. Kim, R. Yetter, F. Dryer, Flow reactor studies and kinetic modeling of the H_2/O_2 reaction, International Journal of Chemical Kinetics 31 (2) (1999) 113–125.

[35] M. A. Mueller, R. Yetter, F. Dryer, Flow reactor studies and kinetic modeling of the $H_2/O_2/NO_x$ and $CO/H_2O/O_2/NO_x$ reactions, International Journal of Chemical Kinetics 31 (10) (1999) 705–724.

[36] J. Li, Z. Zhao, A. Kazakov, M. Chaos, F. L. Dryer, J. J. Scire Jr, A comprehensive kinetic mechanism for CO, CH_2O, and CH_3OH combustion, International Journal of Chemical Kinetics 39 (3) (2007) 109–136.

[37] P. Oßwald, M. Köhler, An atmospheric pressure high-temperature laminar flow reactor for investigation of combustion and related gas phase reaction systems, Review of Scientific Instruments 86 (10).

[38] H. Hashemi, J. M. Christensen, S. Gersen, H. Levinsky, S. J. Klippenstein, P. Glarborg, High-pressure oxidation of methane, Combustion and Flame 172 (2016) 349–364.

[39] M. Alzueta, M. Borruey, A. Callejas, A. Millera, R. Bilbao, An experimental and modeling study of the oxidation of acetylene in a flow reactor, Combustion and flame 152 (3) (2008) 377–386.

[40] T. Carriere, P. Westmoreland, A. Kazakov, Y. Stein, F. Dryer, Modeling ethylene combustion from low to high pressure, Proceedings of the Combustion Institute 29 (1) (2002) 1257–1266.

[41] P. Dagaut, F. Lecomte, J. Mieritz, P. Glarborg, Experimental and kinetic modeling study of the effect of NO and SO_2 on the oxidation of CO-H_2 mixtures, International journal of chemical kinetics 35 (11) (2003) 564–575.

[42] U. Burke, W. K. Metcalfe, S. M. Burke, K. A. Heufer, P. Dagaut, H. J. Curran, A detailed chemical kinetic modeling, ignition delay time and jet-stirred reactor study of methanol oxidation, Combustion and Flame 165 (2016) 125–136.

[43] P. Dagaut, J.-C. Boettner, M. Cathonnet, Methane oxidation: experimental and kinetic modeling study, Combustion science and technology 77 (1-3) (1991) 127–148.

[44] T. L. Le Cong, P. Dagaut, Experimental and detailed kinetic modeling of the oxidation of methane and methane/syngas mixtures and effect of carbon dioxide addition, Combustion Science and Technology 180 (10-11) (2008) 2046–2091.

[45] Y. Tan, P. Dagaut, M. Cathonnet, J.-C. Boettner, Acetylene oxida-

602 tion in a jsr from 1 to 10 atm and comprehensive kinetic modeling,
603 Combustion science and technology 102 (1-6) (1994) 21–55.

604 [46] A. Fomin, T. Zavlev, V. A. Alekseev, A. A. Konnov, I. Rahinov,
605 S. Cheskis, Intracavity laser absorption spectroscopy study of HCO
606 radicals during methane to hydrogen conversion in very rich flames,
607 Energy & Fuels 29 (9) (2015) 6146–6154.

608 [47] A. Fomin, T. Zavlev, V. A. Alekseev, I. Rahinov, S. Cheskis, A. A.
609 Konnov, Experimental and modelling study of $^1CH_2$ in premixed very
610 rich methane flames, Combustion and Flame 171 (2016) 198–210.

611 [48] M. C. Krejci, O. Mathieu, A. J. Vissotski, S. Ravi, T. G. Sikes, E. L.
612 Petersen, K. Alan, W. Metcalfe, H. J. Curran, et al., Laminar flame
613 speed and ignition delay time data for the kinetic modeling of hydrogen
614 and syngas fuel blends, Journal of Engineering for Gas Turbines and
615 Power 135 (2) (2013) 021503.

616 [49] O. Park, P. S. Veloo, H. Burbano, F. N. Egolfopoulos, Studies of
617 premixed and non-premixed hydrogen flames, Combustion and Flame
618 162 (4) (2015) 1078–1094.

619 [50] S. Voss, S. Hartl, C. Hasse, Determination of laminar burning velocities
620 for lean low calorific H_2/N_2 and $H_2/CO/N_2$ gas mixtures, International
621 Journal of Hydrogen Energy 39 (34) (2014) 19810–19817.

622 [51] V. A. Alekseev, A. A. Konnov, Data consistency of the burning ve-
623 locity measurements using the heat flux method: Hydrogen flames,
624 Combustion and Flame 194 (2018) 28–36.

[52] H. Sun, S. Yang, G. Jomaas, C. Law, High-pressure laminar flame speeds and kinetic modeling of carbon monoxide/hydrogen combustion, Proceedings of the Combustion Institute 31 (1) (2007) 439–446.

[53] B. Lohöfener, E. Roungos, S. Voss, D. Trimis, Burning velocities of low calorific value hydrogen and carbon monoxide gas mixtures, in: 2nd Heat Flux Burner Workshop, Warsaw University of Technology, Poland, 2012.

[54] V. R. Kishore, M. Ravi, A. Ray, Adiabatic burning velocity and cellular flame characteristics of H_2–CO–CO_2–air mixtures, Combustion and flame 158 (11) (2011) 2149–2164.

[55] A. A. Konnov, I. V. Dyakov, J. de Ruyck, Nitric oxide formation in premixed flames of H_2 + CO + CO_2 and air, Proceedings of the Combustion Institute 29 (2) (2002) 2171–2177.

[56] L. Sileghem, V. Alekseev, J. Vancoillie, E. Nilsson, S. Verhelst, A. Konnov, Laminar burning velocities of primary reference fuels and simple alcohols, Fuel 115 (2014) 32–40.

[57] A. A. Konnov, I. Dyakov, Nitrous oxide conversion in laminar premixed flames of CH_4 + O_2 + Ar, Proceedings of the Combustion Institute 32 (1) (2009) 319–326.

[58] O. Park, P. S. Veloo, N. Liu, F. N. Egolfopoulos, Combustion characteristics of alternative gaseous fuels, Proceedings of the Combustion Institute 33 (1) (2011) 887–894.

[59] R. T. E. Hermanns, Laminar burning velocities of methane-hydrogen-air mixtures, Ph.D. thesis, Technische Universiteit Eindhoven (2007). doi:10.6100/IR630126.

[60] E. J. Nilsson, A. van Sprang, J. Larfeldt, A. A. Konnov, The comparative and combined effects of hydrogen addition on the laminar burning velocities of methane and its blends with ethane and propane, Fuel 189 (2017) 369–376.

[61] F. Coppens, J. De Ruyck, A. A. Konnov, The effects of composition on burning velocity and nitric oxide formation in laminar premixed flames of $CH_4 + H_2 + O_2 + N_2$, Combustion and Flame 149 (4) (2007) 409–417.

[62] E. Hu, Z. Huang, J. He, J. Zheng, H. Miao, Measurements of laminar burning velocities and onset of cellular instabilities of methane-hydrogen-air flames at elevated pressures and temperatures, International Journal of Hydrogen Energy 34 (13) (2009) 5574 – 5584.

[63] O. Park, P. S. Veloo, F. N. Egolfopoulos, Flame studies of c_2 hydrocarbons, Proceedings of the Combustion Institute 34 (1) (2013) 711–718.

[64] P. Oßwald, R. Whitside, J. Schäffer, M. Köhler, An experimental flow reactor study of the combustion kinetics of terpenoid jet fuel compounds: Farnesane, p-menthane and p-cymene, Fuel 187 (2017) 43 – 50.

[65] C. Olm, I. G. Zsély, T. Varga, H. J. Curran, T. Turányi, Comparison

of the performance of several recent syngas combustion mechanisms, Combustion and Flame 162 (5) (2015) 1793–1812.

[66] Z. Hong, R. D. Cook, D. F. Davidson, R. K. Hanson, A shock tube study of $OH + H_2O_2 \rightarrow H_2O + HO_2$ and $H_2O_2 + M \rightarrow 2OH + M$ using laser absorption of H_2O and OH, The Journal of Physical Chemistry A 114 (18) (2010) 5718–5727.

[67] A. Laskin, H. Wang, On initiation reactions of acetylene oxidation in shock tubes: a quantum mechanical and kinetic modeling study, Chemical Physics Letters 303 (1) (1999) 43–49.

[68] P.-F. Lee, H. Matsui, W.-Y. Chen, N.-S. Wang, Production of H and $O(^3P)$ atoms in the reaction of CH_2 with O_2, The Journal of Physical Chemistry A 116 (37) (2012) 9245–9254.

[69] C. Vinckier, W. Debruyn, Temperature dependence of the reactions of methylene with oxygen atoms, oxygen, and nitric oxide, Journal of physical chemistry 83 (16) (1979) 2057–2062.

[70] M. A. Blitz, C. Kappler, M. J. Pilling, P. W. Seakins, $^3CH_2 + O_2$: Kinetics and product channel branching ratios, Zeitschrift für Physikalische Chemie 225 (9-10) (2011) 957–967.

[71] G. Smith, Y. Tao, H. Wang, Foundational fuel chemistry model version 1.0 (FFCM-1), `http://nanoenergy.stanford.edu/ffcm1` (2016).

[72] C. F. Goldsmith, L. B. Harding, Y. Georgievskii, J. A. Miller, S. J. Klippenstein, Temperature and pressure-dependent rate coefficients for

the reaction of vinyl radical with molecular oxygen, The Journal of Physical Chemistry A 119 (28) (2015) 7766–7779.

[73] T. Kathrotia, U. Riedel, J. Warnatz, A numerical study on the relation of oh*, ch*, and c2* chemiluminescence and heat release in premixed methane flames, in: Proceedings of the European combustion Meeting, Citeseer, 2009, pp. 1–5.

[74] T. Kathrotia, M. Fikri, M. Bozkurt, M. Hartmann, U. Riedel, C. Schulz, Study of the h+ o+ m reaction forming oh: Kinetics of oh chemiluminescence in hydrogen combustion systems, Combustion and Flame 157 (7) (2010) 1261–1273.

[75] B. Ruscic, D. H. Bross, Active Thermochemical Tables (ATcT) values based on version 1.122 of the Thermochemical Network, available at `ATcT.anl.gov`.

[76] P. Glarborg, J. A. Miller, B. Ruscic, S. J. Klippenstein, Modeling nitrogen chemistry in combustion, Progress in Energy and Combustion Science 67 (2018) 31–68.

[77] Z. Hong, D. F. Davidson, R. K. Hanson, An improved H_2/O_2 mechanism based on recent shock tube/laser absorption measurements, Combustion and Flame 158 (4) (2011) 633–644.

[78] A. Kéromnès, W. K. Metcalfe, K. A. Heufer, N. Donohoe, A. K. Das, C.-J. Sung, J. Herzler, C. Naumann, P. Griebel, O. Mathieu, M. C. Krejci, E. L. Petersen, W. J. Pitz, H. J. Curran, An experimental and detailed chemical kinetic modeling study of hydrogen and syngas

mixture oxidation at elevated pressures, Combustion and Flame 160 (6) (2013) 995 – 1011.

[79] J. Troe, V. Ushakov, The dissociation/recombination reaction CH_4 (+ M) $\leftrightarrow$ CH_3 + H (+ M): A case study for unimolecular rate theory, The Journal of chemical physics 136 (21) (2012) 214309.

[80] N. Faßheber, G. Friedrichs, P. Marshall, P. Glarborg, Glyoxal oxidation mechanism: implications for the reactions HCO + O_2 and OCHCHO + HO_2, The Journal of Physical Chemistry A 119 (28) (2015) 7305–7315.

[81] S. J. Klippenstein, J. A. Miller, L. B. Harding, Resolving the mystery of prompt CO_2: The HCCO + O_2 reaction, Proceedings of the Combustion Institute 29 (1) (2002) 1209–1217.

[82] A. W. Jasper, S. J. Klippenstein, L. B. Harding, B. Ruscic, Kinetics of the reaction of methyl radical with hydroxyl radical and methanol decomposition, The Journal of Physical Chemistry A 111 (19) (2007) 3932–3950.

[83] A. W. Jasper, S. J. Klippenstein, L. B. Harding, Theoretical rate coefficients for the reaction of methyl radical with hydroperoxyl radical and for methylhydroperoxide decomposition, Proceedings of the Combustion Institute 32 (1) (2009) 279–286.

[84] Z. Xu, P. Raghunath, M. Lin, Ab initio chemical kinetics for the ch3+ o (3p) reaction and related isomerization–decomposition of ch3o and ch2oh radicals, The Journal of Physical Chemistry A 119 (28) (2015) 7404–7417.

[85] S. Dóbé, T. Bérces, I. Szilágyi, Kinetics of the reaction between methoxyl radicals and hydrogen atoms, Journal of the Chemical Society, Faraday Transactions 87 (15) (1991) 2331–2336.

[86] S. Wang, D. F. Davidson, R. K. Hanson, Improved shock tube measurement of the CH_4 + Ar = CH_3 + H + Ar rate constant using UV cavity-enhanced absorption spectroscopy of CH_3, The Journal of Physical Chemistry A 120 (28) (2016) 5427–5434.

[87] P. Frank, K. Bhaskaran, T. Just, Acetylene oxidation: The reaction c2h2+ o at high temperatures, in: Symposium (International) on Combustion, Vol. 21, Elsevier, 1988, pp. 885–893.

[88] J. P. Senosiain, S. J. Klippenstein, J. A. Miller, The reaction of acetylene with hydroxyl radicals, The Journal of Physical Chemistry A 109 (27) (2005) 6045–6055.

[89] J. A. Miller, S. J. Klippenstein, The H + C_2H_2 (+ M) $\rightleftharpoons$ C_2H_3 (+ M) and H + C_2H_2 (+ M) $\rightleftharpoons$ C_2H_5 (+ M) reactions: Electronic structure, variational transition-state theory, and solutions to a two-dimensional master equation, Physical Chemistry Chemical Physics 6 (6) (2004) 1192–1202.

[90] X. Li, A. W. Jasper, J. Zádor, J. A. Miller, S. J. Klippenstein, Theoretical kinetics of O + C_2H_4, Proceedings of the Combustion Institute 36 (1) (2017) 219–227.

[91] E. Ranzi, A. Frassoldati, R. Grana, A. Cuoci, T. Faravelli, A. Kelley, C. Law, Hierarchical and comparative kinetic modeling of laminar

760 flame speeds of hydrocarbon and oxygenated fuels, Progress in Energy
761 and Combustion Science 38 (4) (2012) 468–501.

762 [92] Y. Li, C.-W. Zhou, K. P. Somers, K. Zhang, H. J. Curran, The oxida-
763 tion of 2-butene: A high pressure ignition delay, kinetic modeling study
764 and reactivity comparison with isobutene and 1-butene, Proceedings of
765 the Combustion Institute 36 (1) (2017) 403–411.

766 [93] D. G. Goodwin, H. K. Moffat, R. L. Speth, Cantera: An object-oriented
767 software toolkit for chemical kinetics, thermodynamics, and trans-
768 port processes, `http://www.cantera.org`, version 2.3.0 (11 2017).
769 doi:10.5281/zenodo.170284.

770 [94] E. Agelidou, T. Monz, A. Huber, M. Aigner, Experimental investiga-
771 tion of an inverted brayton cycle micro gas turbine for chp application,
772 in: ASME Turbo Expo 2017: Turbomachinery Technical Conference
773 and Exposition, no. GT2017-64490, American Society of Mechanical
774 Engineers, 2017, p. V008T26A023.

775 [95] W.-D. Hsieh, R.-H. Chen, T.-L. Wu, T.-H. Lin, Engine performance
776 and pollutant emission of an si engine using ethanol–gasoline blended
777 fuels, Atmospheric Environment 36 (3) (2002) 403–410.

778 [96] J. J. Scire Jr, R. A. Yetter, F. L. Dryer, Flow reactor studies of methyl
779 radical oxidation reactions in methane-perturbed moist carbon monox-
780 ide oxidation at high pressure with model sensitivity analysis, Interna-
781 tional Journal of Chemical Kinetics 33 (2) (2001) 75–100.

[97] Z. Hong, D. F. Davidson, K.-Y. Lam, R. K. Hanson, A shock tube study of the rate constants of HO_2 and CH_3 reactions, Combustion and Flame 159 (10) (2012) 3007–3013.

[98] N. Srinivasan, J. Michael, L. Harding, S. Klippenstein, Experimental and theoretical rate constants for $CH_4 + O_2 \rightarrow CH_3 + HO_2$, Combustion and flame 149 (1-2) (2007) 104–111.

[99] D. Davidson, R. Hanson, C. Bowman, Revised values for the rate coefficients of ethane and methane decomposition, International journal of chemical kinetics 27 (3) (1995) 305–308.

[100] W. Shaub, D. Hsu, T. Burks, M. Lin, Dynamics and mechanisms of CO production from the reactions of CH_2 radicals with O (3P) and O_2, in: Symposium (International) on Combustion, Vol. 18, Elsevier, 1981, pp. 811–818.

[101] A. O. Langford, H. Petek, C. B. Moore, Collisional removal of $CH_2(^1A_1)$: Absolute rate constants for atomic and molecular collisional partners at 295 k, The Journal of Chemical Physics 78 (11) (1983) 6650–6659.

[102] G. Hancock, V. Haverd, A time-resolved ftir emission study of the gas phase removal processes of $CH_2(X^3B_1)$ and $CH_2(a^1A_1)$ in collisions with O_2, Chemical physics letters 372 (1-2) (2003) 288–294.